Åbo Akademi

OPEN ACCESS

This is an electronic reprint of the original article. This reprint may differ from the original in pagination and typographic detail.

Epoxidation of vegetable oils in a semibatch reactor: From reaction kinetics to reactor modelling

Tolvanen, Pasi; Eränen, Kari; Wärnå, Johan; Freites, Adriana; Kilpiö, Teuvo; Salmi, Tapio

Published in:
Chemical Engineering Research and Design

DOI:
10.1016/j.cherd.2026.03.002

Published: 01/04/2026

Document Version
Final published version

Document License
CC BY

Link to publication

Please cite the original version:
Tolvanen, P., Eränen, K., Wärnå, J., Freites, A., Kilpiö, T., & Salmi, T. (2026). Epoxidation of vegetable oils in a semibatch reactor: From reaction kinetics to reactor modelling. *Chemical Engineering Research and Design*, *228*, 265-278. https://doi.org/10.1016/j.cherd.2026.03.002

General rights
Copyright and moral rights for the publications made accessible in the public portal are retained by the authors and/or other copyright owners and it is a condition of accessing publications that users recognise and abide by the legal requirements associated with these rights.

Take down policy
If you believe that this document breaches copyright please contact us providing details, and we will remove access to the work immediately and investigate your claim.

This document is downloaded from the Research Information Portal of ÅAU: 24. Nov. 2026

Chemical Engineering Research and Design 228 (2026) 265–278

Contents lists available at ScienceDirect

Chemical Engineering Research and Design

journal homepage: www.elsevier.com/locate/cherd

Epoxidation of vegetable oils in a semibatch reactor: From reaction kinetics to reactor modelling

Pasi Tolvanen, Kari Eränen, Johan Wärnå, Adriana Freites, Teuvo Kilpiö, Tapio Salmi *

Åbo Akademi, Johan Gadolin Process Chemistry Centre (PCC), Laboratory of Industrial Chemistry and Reaction Engineering (TKR), Turku/Åbo FI-20500, Finland

ARTICLE INFO

Keywords:
Epoxidation
Vegetable oil
Semibatch reactor
Yield optimization
Kinetics
Mathematical modelling

ABSTRACT

Epoxidized vegetable oils are used as green intermediates in organic synthesis as well as biolubricants and plasticizers. Epoxidation of double bonds in a commercial vegetable oil mixture was carried out in a laboratory-scale semibatch reactor, which was operated at 25–30 °C and at atmospheric pressure. Potassium persulphate was used as the oxidation agent and potassium hydroxide was added to the reaction mixture to maintain the pH constant. An extensive experimental optimization of the reaction conditions (oxidant-to-double bond ratio and oxidant feed rate) was carried out, revealing that more than 95% of the double bonds could be epoxidized in the best cases. The experiments provided a large set of kinetic data which were modelled mathematically. Mathematical expressions for the epoxidation rate were derived, based on plausible reaction mechanisms and on the principle of quasi-stationarity for the reaction intermediates appearing in the molecular mechanism of the double bond epoxidation. The kinetic parameters in the mathematical model, a set of ordinary differential equations for the components in the semibatch reactor, were determined by non-linear regression analysis. A comparison of the model predictions with experimental data revealed that the model described the epoxidation kinetics of vegetable oils in the isothermal and isobaric semibatch reactor very well.

1. Introduction

Vegetable oils are traditionally used by human households due to the nutritional values and the apparent health benefits originated from the oil's high content of free fatty acids, such as the conjugated omega acids, which are claimed to promote weight loss and reduce cardiovascular diseases (Funck et al., 2006) (Funck et al., 2006). Naturally, vegetable oils do not consist of "free" fatty acids, but instead they exist in triglycerides, i.e. three fatty acids are connected to a glycerol backbone. The length of a fatty acid can vary significantly (4–28 carbon chain length), as can the amount of double bonds (= unsaturation), and therefore the number of different fatty acids is large. However, the vegetable oils consist of a merely narrow fatty acid distribution. Rapeseed is the third largest source of vegetable oil, after soybean and oil palm, and is used mostly for animal feed, vegetable oil for human consumption, and for the production of biodiesel.

In addition to their nutritional and energy uses, vegetable oils have gained significant attention as renewable feedstocks in green chemical synthesis, particularly through functionalization such as epoxidation. Epoxides are very important building blocks in organic synthesis due to their high reactivity and versatility in forming a wide range of functionalized compounds, such as flavors, adhesives, fragrances, paints, and pharmaceuticals. The epoxide group is more reactive than a double bond, thus providing a more energetically favorable site for reaction. Recent developments have increasingly focused on greener epoxidation methods, including the use of bio-based oxidants and heterogeneous catalysts to support more sustainable chemical manufacturing (Saurabh, 2011). In particular, the epoxidation of fatty acid double bonds in vegetable oils leads to cyclic ethers that serve as environmentally friendly biodegradable alternatives to petrochemical-derived intermediates. These epoxidized vegetable oils can be further transformed into polyols, glycols, carbonyl compounds as well as lubricants and plasticizers, instead of relying on products derived from petrochemical industry (Saurabh, 2011; Goering et al., 1982; Hanif et al., 2024; Meng et al., 2021; Mohammed and Saha, 2022).

Vegetable oil can be epoxidized by using acidic ion exchange resins, enzymes, or metal catalysts (Adhvaryu and Erhan, 2002; Campanella and Baltanás, 2007; Campanella et al., 2008, 2010; Goud et al., 2007a, 2007b; Hilker et al., 2001; Lathi and Mattiasson, 2007; Santacesaria

Abbreviations: A, oxidant, here: Caroat; B, solvent and catalyst, here: acetone; C, vegetable oil, double bond; DMDO, dimethyldioxirane DMDO = I; I, I_1, I_2, reaction intermediate; IV, iodine number; OH, hydroxide, here: KOH; P, oxirane, epoxidized double bond; S, product salt, here K_2SO_4; W, water.

* Corresponding author.
E-mail address: tapio.salmi@abo.fi (T. Salmi).

https://doi.org/10.1016/j.cherd.2026.03.002
Received 7 January 2026; Received in revised form 19 February 2026; Accepted 2 March 2026
Available online 3 March 2026
0263-8762/© 2026 The Authors. Published by Elsevier Ltd on behalf of Institution of Chemical Engineers. This is an open access article under the CC BY license (http://creativecommons.org/licenses/by/4.0/).

Notation

a	merged parameter in rate equation
c	concentration
K	equilibrium constant
k,k',k'',k'''	rate constant
m	mass
N	normality
n	amount of substance
Q	objective function
r	rate
t	time
V	volume
$\dot{V}$	volumetric flow rate
α	merged rate parameter
ϰ	empirical exponent

Subscripts

i, j	component indices, j refers particularly to a component fed into the semibatch reactor

et al., 2011; Törnvall et al., 2007). However, the most common way to perform the epoxidation reaction on an industrial scale is to use in situ formed peracids combined with a carboxylic acid as an oxygen carrier. In recent years, process intensification tools such as microwave (MW) and ultrasound (US) irradiation have also been explored to enhance the performance of the Prilezhaev epoxidation. US has been shown to improve epoxidation yields by enhancing mass transfer and cleaning the surface of immobilized enzyme particles, while MW-assisted systems have demonstrated benefits from selective heating and reduced reaction times (Aguilera et al., 2022, 2018, 2019). Despite their widespread use, conventional epoxidation methods present important limitations. The classical Prilezhaev approach, which relies on in situ formed peracids, suffers from corrosiveness and notable safety concerns due to strong exothermicity and the potential for hazardous decomposition, especially at industrial scale (Leveneur et al., 2018). Enzyme-catalyzed epoxidation, while milder and more environmentally friendly, is often limited by high catalyst cost, reduced operational stability, and slower reaction rates. Diffusion constraints and sensitivity to reaction conditions (e.g., pH or oxidant concentration) can further hinder efficiency, particularly with viscous substrates like vegetable oils. These challenges have motivated the search for alternative oxidant systems that combine safety, efficiency, and process control. One such approach involves the use of triple salts such as Caroat® or Oxone® (potassium monopersulfate-based oxidants) in combination with a ketone like acetone offers a powerful route to epoxidation via in situ generation of dimethyldioxirane (DMDO), a highly reactive and selective oxygen-transfer species (Shu and Shi, 2000). Originally developed by Shu and co-workers in 2000, this method has been widely applied to the epoxidation of small alkenes and fine chemicals under mild, green conditions. However, despite its versatility, there are to date no comprehensive studies reported on the use of this oxidant system for the epoxidation of vegetable oils or related long-chain fatty derivatives. In this work, we explore the application of Caroat-based epoxidation for vegetable oil substrates under semibatch conditions. The study builds on a prior patented concept (Lämsä and Kosonen, 2012) that demonstrated the feasibility of using potassium peroxymonosulfate and ketone systems for vegetable oil epoxidation at laboratory scale. Here, we extend that work by investigating the detailed reaction kinetics, optimizing yield, and evaluating reactor operation under controlled semibatch conditions. Acetone participates in the formation of DMDO and is regenerated after the reaction, contributing to the sustainability of the system. Additionally, the pH is maintained at a slightly alkaline level throughout the reaction to facilitate DMDO formation. However, a too alkaline solution must be avoided to prevent saponification of the oil. Therefore, KOH is continuously fed into the reactor to maintain the pH level. The oxidant, Caroat, is also added gradually as an aqueous solution to the reactor, due to its high acidity and solid crystalline nature. Caroat is solid crystalline in nature, and must therefore be dissolved in water prior to the addition. The Caroat solution used was nearly saturated to minimize the overall reaction volume. The solubility of Caroat is approximately 256 g in 1 liter of water at room temperature. A 1 wt.-% solution of Caroat has approximately pH= 2.2. As a result, the reaction system is a relatively complex, with several components added to the reactor in a semibatch-wise manner. The cyclic reaction mechanism for

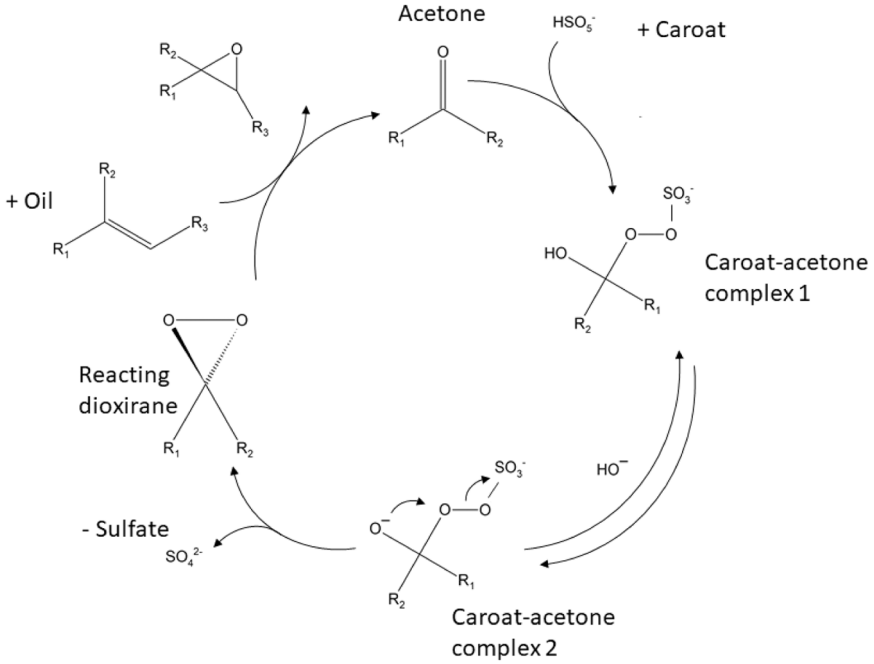


Fig. 1. An illustration of the Caroat-acetone reaction cycle proposed by Shu and Shi (2000) (Shu and Shi, 2000).

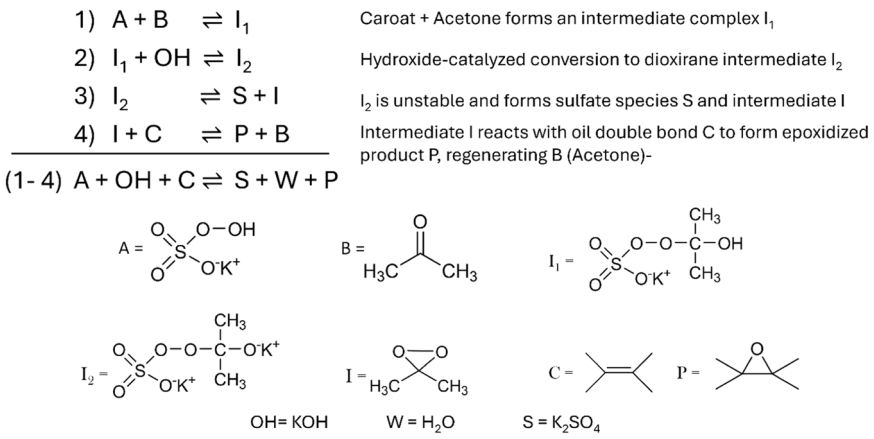


Fig. 2. The molecular structure of Caroat (A), acetone (B), the oils' double bonds (C), and their intermediates (I, I_1, I_2,) and the product, epoxidized double bond on the oil (P). The reaction scheme is based on Fig. 1.

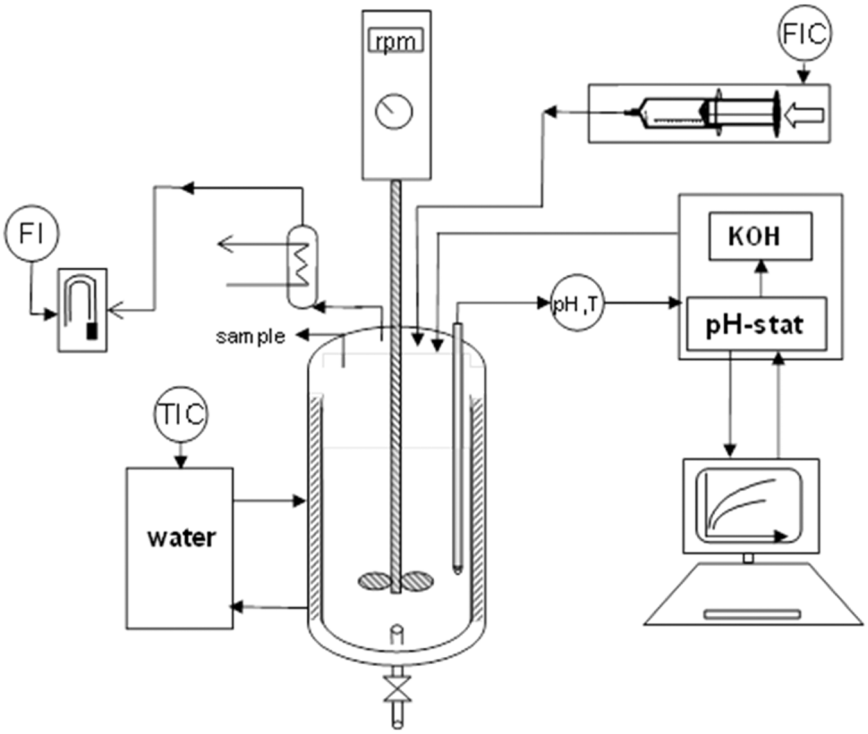


Fig. 3. Experimental equipment for vegetable oil epoxidation. FI = flow indicator, FIC = flow indicator and controller, TIC = Temperature indicator and controller.

the vegetable oil epoxidation in the Caroat-acetone system is illustrated in Fig. 1, which shows the key reactive intermediates. Based on the mechanism, a more detailed reaction scheme is presented in Fig. 2.

As can be seen from Fig. 1, the Caroat triple salt, peroxy monosulfate, first forms a complex dimethyldioxirane (DMDO), with acetone, which is the active component. Basically, any ketone would do the job, but acetone has found to be a safe, rather inexpensive, and moreover, an excellent solvent for vegetable oils. A too low pH would lead to a Bayer-Villiger type oxidation of acetone, and therefore the pH is regulated with continuous alkaline addition.

The aim of this study was to optimize different reaction parameters such as the molar ratios of oxidant-to-double bonds, the amount of acetone, and the oxidant feed rate, in order to maximize the yield of the epoxidized oil, and to minimize the ring opening of the product and the formation of other by-products, and to minimize the volume of the reaction medium.

2. Experimental section

2.1. Epoxidation experiments

Kinetic experiments were performed in a jacketed cylindrical glass reactor (total volume 1.0 L), equipped with a mechanical stirrer. Different stirrers were preliminary evaluated, and showed no significant influence on the observed reaction rates. Consequently, a standard propeller stirrer was selected for all systematic experiments. A constant stirring speed of 600 rpm was applied to ensure operation under conditions where mass transfer limitations were negligible and intrinsic kinetics prevailed. Agitation was provided by an overhead stirrer (Heidolph RZR 2021). Commercial rapeseed oil was used as substrate in all experiments without further purification. The reaction temperature was controlled by recirculation of water through the reactor jacket. A nearly saturated Caroat solution was prepared immediately prior to each experiment. A schematic representation of the experimental setup is

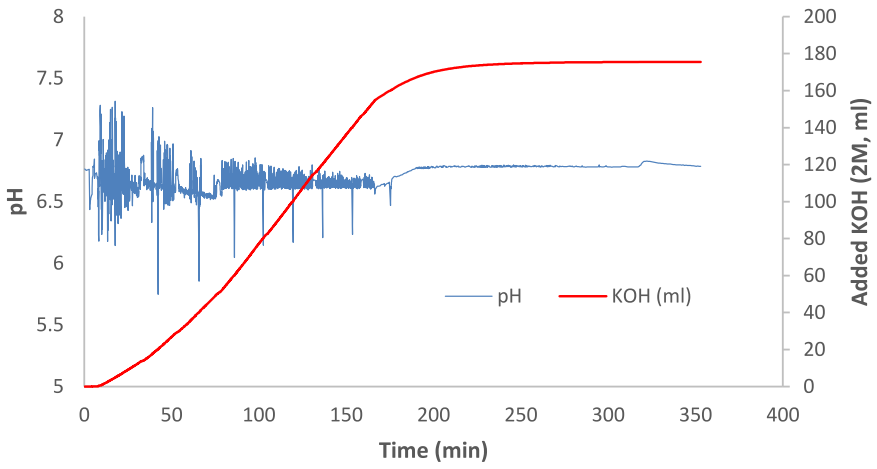


Fig. 4. The pH and KOH consumption curves from an epoxidation experiment with a Caroat feed rate of 120 ml/h, resulting in a total oxidant addition time of approximately 165–170 min.

illustrated in Fig. 3.

From iodometric analysis, it was found out that 63.10 g of Caroat (in form of pure K salt, component A in Fig. 2) was needed to epoxidize all double bonds (DB) in 40.00 g of rapeseed oil. Typically, experiments with 40 g of oil were performed and the Caroat amount was thereafter calculated in respect to which oxidant-to- double bond ratio was needed. The acetone amount was typically 4.5 mol per mol DB. In some experiments, different amounts of both oil and acetone were used. In this work, molar ratios in the range of 0.5–2.0 of Caroat were used in respect to the amount of DB. These molar ratios are given on an overall basis, referring to the total amount of oxidant added over the full course of the reaction, rather than to instantaneous concentrations during the dropwise addition. This basis was also used consistently in the kinetic modeling. The Caroat solution was injected dropwise from a 60 ml plastic syringe (Plastipak 50), and controlled by a precision pump (Alaris Asena GS), with which the flow rate was maintained in the range of 5–300 ml/h. The syringe was quickly filled again as the solution was close to end, until all Caroat had been fed into the reactor. After this stage, the reaction was still allowed to proceed to ensure that all oxidant had been consumed.

Normally, it was possible to follow the reaction indirectly by monitoring the KOH consumption, which follows quite linearly with the reaction – when no Caroat was left in the reactor, the consumption of alkaline declined (see Fig. 4). A pH-stat device (Metrohm799 GPT Tiamo, pH electrode Metrohm 6.0248.020 pH 0…14/0…100°C, Pt 1000/B/2/3 M KCl) was used to control the pH at desired level by continuous addition of KOH (1.0–5 M). The reactor setup also featured a condenser (<10 °C) on the top of reactor. The temperature in the reactor was typically kept constant in the range of 25–30°C, since higher temperatures increase the ring opening and moreover, does not enhance the reaction rate significantly.

Samples (10–15 ml) were withdrawn through a hole on the reactor top with a plastic syringe, and the product phases were quickly separated by settling, washing with hot water and the oil phase was furthermore purified from excess water by the addition of sodium sulphate. Typically, only three samples were taken per experiment: one at the midpoint of the Caroat feed, one immediately after the feed ended, and one final sample at the end of the reaction. Of these, only the midpoint sample overlapped with the semibatch addition phase and was therefore potentially influential on the reaction balance. However, the oil content in each sample was only about 1.7 g out of the initial 40 g, corresponding to approximately 3.7% of the total oil charge. This was sufficient for accurate oxirane titration while having negligible impact on reaction stoichiometry. Moreover, capturing this intermediate point was important for understanding the kinetic profile during the semibatch phase. By this procedure, a final amount of approximately 1.7 g of dried epoxidized oil per sample was obtained for quantitative product analysis. A white, sometime slightly yellowish product was obtained, which rather quickly solidified if the product yield was high enough. A typical reaction sample showing the upper oil layer and aqueous phase is provided in the Supplementary Information (Figure S5), illustrating the need for sufficient sampling volume to recover analyzable quantities of oil.

2.2. *Analysis procedures*

The molecular structures of vegetable oils differ significantly, depending on their origin. Some oils may be rich in low-molecular fatty acids, whereas others may be the opposite. In the case of rapeseed oil, the largest fatty acid fraction consists of the unsaturated C18 fatty acids, i.e. oleic acid (64 wt.-%), linoleic (2 wt.-%) acid and linolenic acid (8 wt.-%) (Hanif et al., 2024). However, every batch may differ significantly and therefore the iodine value (IV), which expresses the amount of double bonds present in the oil, was analyzed in the unmodified and modified oils. The oxirane oxygen content of the epoxidized samples was determined according to AOCS Official Method Cd 9–57, while the iodine value was measured using the Hanus method, following the procedure equivalent to AOCS Cd 1–25. These are both established analytical standards. Additional details on the reagents, sample handling, and titration setup are provided in the Supplementary Information.

For selected samples, product structures were analyzed using both NMR and GC-MS. In the ˆ1H NMR spectra, signals corresponding to epoxy groups (around 3.0 ppm) and unreacted double bonds (around 5.5 ppm) were clearly observed, while no peaks indicating ring-opened side products such as hydroxyl groups were detected. GC-MS analysis was performed to further investigate product composition, but direct analysis of the epoxidized oil was not feasible due to its non-volatile, polar, and thermally unstable nature. Therefore, a hydrolysis step was carried out to cleave the triglyceride backbone and generate smaller, more volatile methyl ester derivatives suitable for gas-phase separation. This step enabled effective chromatographic analysis but also led to partial conversion of epoxide moieties into methoxy derivatives, slightly complicating interpretation. Derivatization was not applied due to concerns regarding the stability of epoxides under typical derivatization conditions. Full NMR and GC-MS spectra, along with calibration details, will be included in the Supplementary Information.

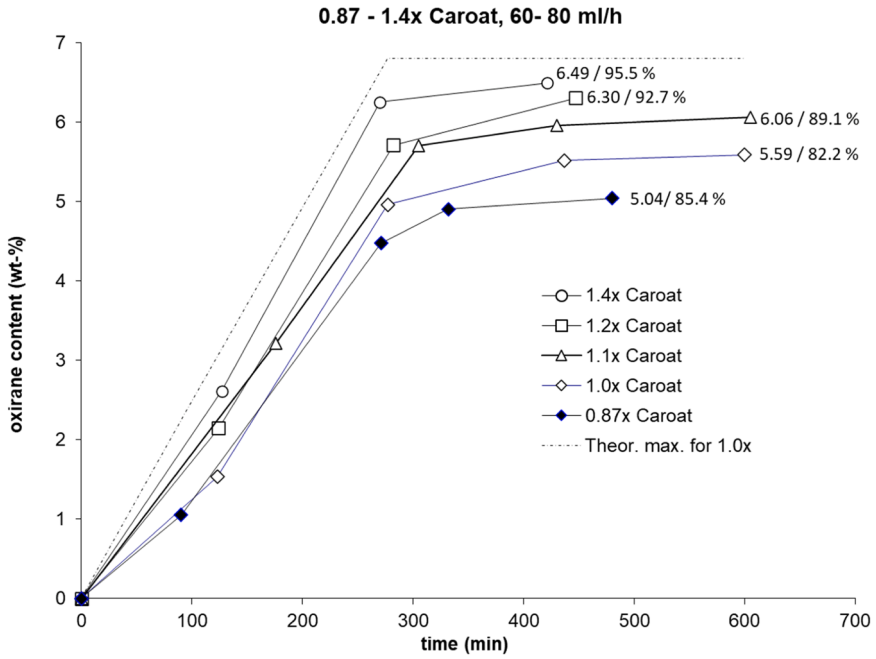


Fig. 5. Oxirane formation over time under different stoichiometric Caroat amounts (0.87–1.4 ×) at a fixed dosage flow of 60 ml/h. Labels at the final data points indicate the final oxirane content (left value, wt%) and corresponding epoxide yield relative to theoretical maximum (right value, %), formatted as oxirane / yield (e.g., 6.30 / 92.7%). This labeling format is used consistently across all similar figures (Figs. 5, 7, 9 and 11).

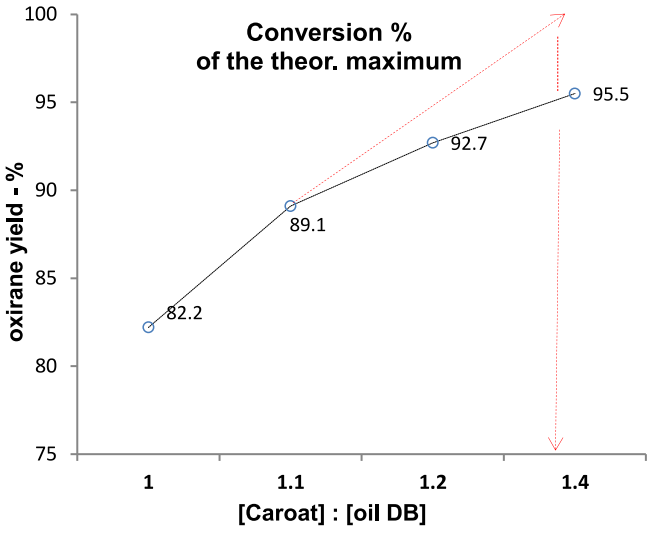


Fig. 6. The influence of the Caroat (A):oil double bonds molar ratio on the oxirane (P) yield %.

3. Experimental results

3.1. The effect of oxidant amount

The Caroat amount was varied in relation to available double bonds (DB) in the oil (Fig. 5). The iodine value of the used rapeseed oil was calculated to be IV = 117. Based on this, it was calculated that the theoretical maximum oxirane value was 6.80. The standard Caroat feed rate was 60 ml/h, and the standard oil amount was 40 g (=0.185 mol DB). Thus the total amount of Caroat was 63.10 g (0.185 mol), and it was dissolved in 270 ml water which gave a total oxidant solution of 310 ml. Therefore, the total time required to titrate the oxidant to the reactor at a rate of 60 ml/h was approximately 5 h. After the addition period, the experiment was continued until no alkaline solution was needed to maintain the pH at the desired level (typically pH =6.80). The standard acetone amount was 4.5 times the amount of DB, which was equal to 58 g when using 40 g of oil. Detailed stoichiometric calculations and iodine value comparisons supporting these conditions are provided in the Supplementary Information.

It is important to note that the epoxide yield is calculated relative to the limiting reagent in each experiment. In cases where Caroat is sub-stoichiometric (e.g., 0.87 ×), the yield reflects the efficiency of oxidant use and can appear high, even though not all double bonds are epoxidized. Conversely, when Caroat is in excess, the yield is based on the theoretical maximum from the oil's double bond content. This normalization ensures that the reported yields reflect efficiency within the actual reagent ratio used. When using the molar ratio Caroat (A): DB = 1:1 and 60 ml/h feed rate, it was observed that the actual oxirane value was significantly lower (5.59) than the theoretical maximum (6.80), reaching a yield of only 82%, see Figs. 5 and 6. By increasing the excessive amount of Caroat to 1.20x, the oxirane yield increased from 82% to 89%, whereas increasing the excess to even higher, the increase of the yield retarded in a nonlinearly manner. Theoretically, with a linear relationship, the excess of 1.30x Caroat would have given 100% yield as illustrated with the red arrow in Fig. 6. Therefore, it was suspected that part of the Caroat is lost due to unproductive side reactions or self-decomposition, especially under alkaline and organic-rich conditions. While this has not been directly measured, the reaction behavior and yield data suggest such losses could contribute to the observed inefficiency. These hypotheses will be further discussed in Section 4.1.

Additionally, a small amount of white residue was occasionally observed adhering to the reactor walls after the experiments. This was likely composed of potassium salts such as K_2SO_4, potentially formed through slow decomposition of Caroat in the presence of the continuously added KOH. Although the system was maintained at near-neutral pH (~7.0), even mild alkalinity may contribute to gradual oxidant degradation. This residue did not interfere with sampling or phase separation but may represent a side pathway that competes with epoxidation and helps explain why full oxidant-to-epoxide conversion was not achieved.

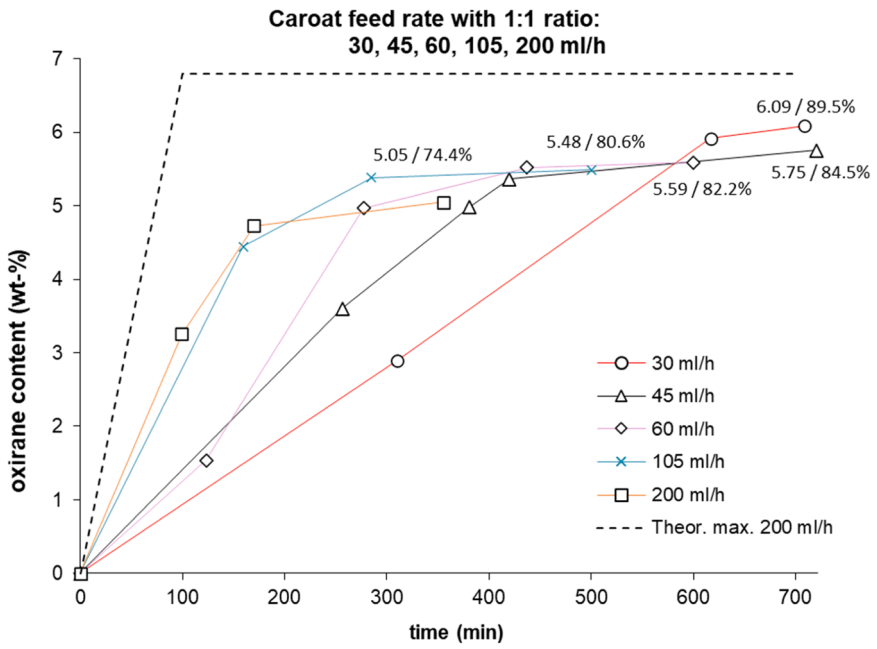


Fig. 7. The influence of the Caroat (A) feed rate on the oxirane (P) formation when using the reactant ratio A:C = 1:1.

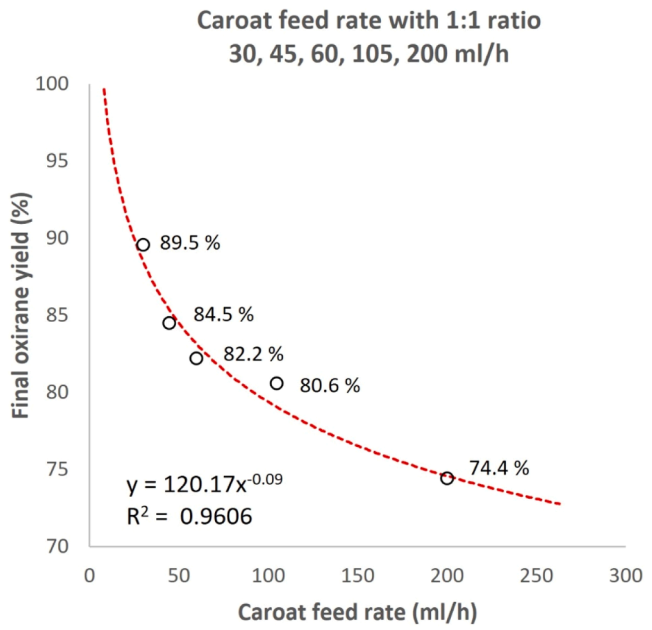


Fig. 8. Influence of Caroat feed rate (30–200 ml/h) on final oxirane content (wt%) for reactions conducted with a 1:1 molar ratio of Caroat to oil double bonds. A power-law trendline is shown for visualization.

3.2. *The influence of Caroat feed rate on the oxirane yield*

The observation of that a 100% oxirane yield could not be obtained even with a large excess of Caroat, lead to the conclusion that part of the Caroat is decomposed during the reaction. Apparently, the reaction solution became too rich of Caroat due to a too rapid addition, and hence presumably either reacting with itself, or, the intermediate, DMDO (I, see Fig. 2), which is in gas form, escaped the reactor setup. A slower feed rate of Caroat would therefore keep the intermediate concentration at a low level, and might thus lead to a higher conversion. Therefore, a set of experiments was performed to reveal the effect of the Caroat feed rate.

3.2.1. *Feed rate experiments with the Caroat: double bond ratio 1:1*

In this set of experiments, 40 g of oil, 59 g of acetone and 63 g of Caroat were used. The pH was kept constant at 6.8 and the Caroat feed used were 30, 45, 60, 105 and 200 ml/h, see Fig. 7. After the addition of all the Caroat solution, the experiments were continued for additional 2–4 h. Consequently, the fastest addition (200 ml/h) experiment was also the shortest by total length, 1.5 h+ 4 h, while the longest was with the slowest addition (30 ml/h), 10 h+ 2 h.

It can be seen from Fig. 7, that the Caroat feed rate highly influences the final oxirane yield, in the direction that the slower feed rate, the higher oxirane yield is obtained. With a high feed rate such as 105 ml/h and 200 ml/h, the reaction proceeds very rapidly, as can be seen at early samples taken at 100 min when all Caroat (300 ml) had been injected, but the final result is the poorest, with a oxirane yield of only 74.4%. The feed rates 105 ml/h and 200 ml/h give practically the same initial rate, but the final oxirane yield is somewhat higher for 105 ml/h. The best yield was obtained with 30 ml/h, the slowest feed rate performed. The change of the final oxirane yield as a function of the feed rate, which possesses an exponential shape, is illustrated in Fig. 8. However, not even with 30 ml/h, could the oxirane yield be increased to a highest possible level (exceeding 90%), and therefore a similar set of experiments, the amount of Caroat was increased to an excess amount of 1.2x, see Section 3.2.2.

Fig. 8 opens a perspective for process optimization and intensification. The production capacity is proportional to y/t where y is the yield and t is the total feeding time. Because the total amount of Caroat is constant, the feeding time is inversely proportional to the feed rate (x in Fig. 8). This implies that the objective function can be formulated as y*x. After inserting the y-function from Fig. 6, we get the objective function ($120.17*x0.^{91}$) which is a monotonically increasing function. The highest possible feeding rate is determined by the product quality criterion, i.e. the yield required. For example, if an oxirane yield of 85% is required, the feeding rate should be 50 ml/h, or less (Fig. 8). The objective function gets its highest value at this boundary. In this way, Fig. 8 can be used for searching the highest possible production capacity within the constraint of the yield required.

3.2.2. *Feed rate experiments with an excess amount of Caroat*

Since a part of Caroat seemed to decompose during the reaction, an excess (10% and 20%) of it was used. Similarly to the experiments

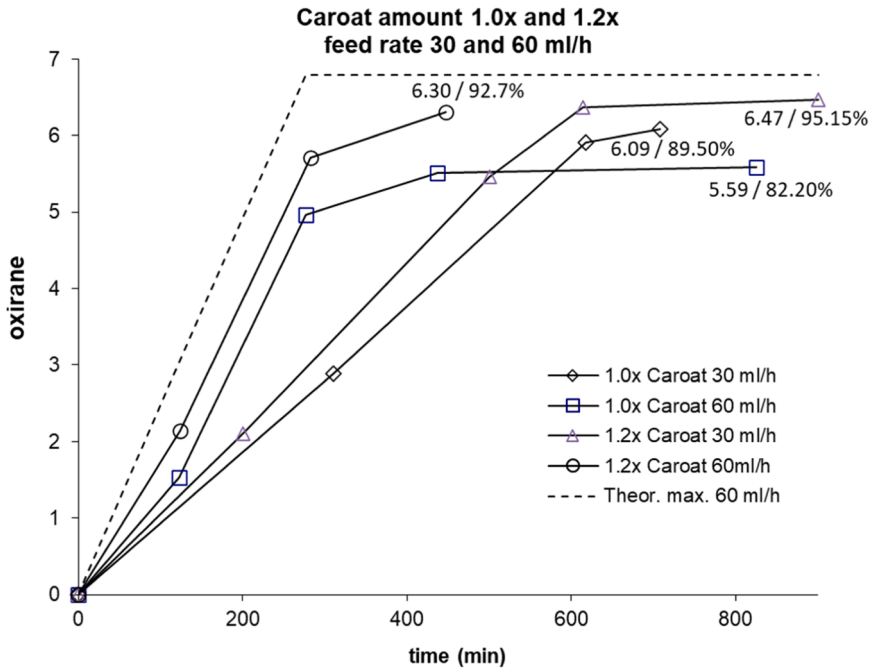


Fig. 9. Comparison of using Caroat (A) amounts 1.2x /1.0x and feed rates 30 /60 ml/h.

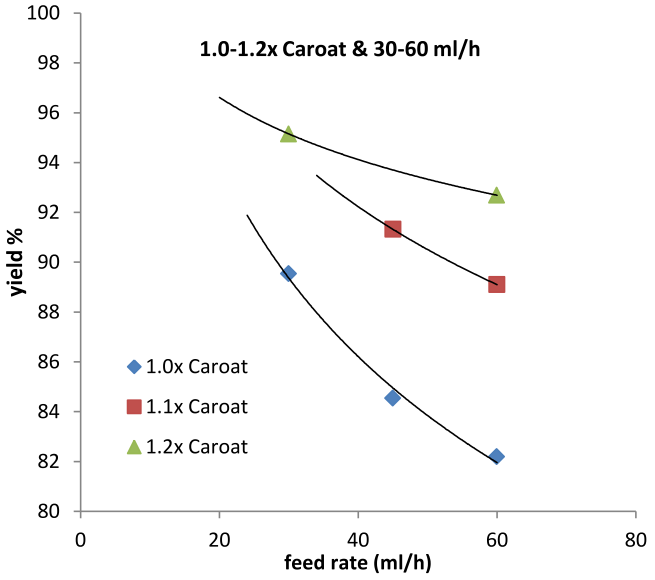


Fig. 10. Effect of Caroat feed rate (30–60 ml/h) on oxirane yield (%) at three different Caroat-to-double bond molar ratios (1.0x, 1.1x, and 1.2x). Power-law trendlines are included for visual guidance.

reported in Section 3.2.1, the Caroat feed rates of 30, 45 and 60 ml/h were used. By increasing the Caroat amount, it was found out that the epoxy yield was further increased, however 100% yield was still not obtained, see Fig. 9. By using 20% excess Caroat, the final yield was increased from 89.5% to 95.5%, when using the slowest feed rate 30 ml/h. Note that since more Caroat was used, also the total feed time was consequently longer. This however, should not influence the interpretation of the results. The increase of the epoxy yield as a function of the feed rates using excess amounts of Caroat is more clearly illustrated in Fig. 10. It could be imagined, that if reducing the feed rate close to zero ml/h, the all the yields with different excess amounts would coincide at the 100% mark.

3.3. The influence of pH on the oxirane yield

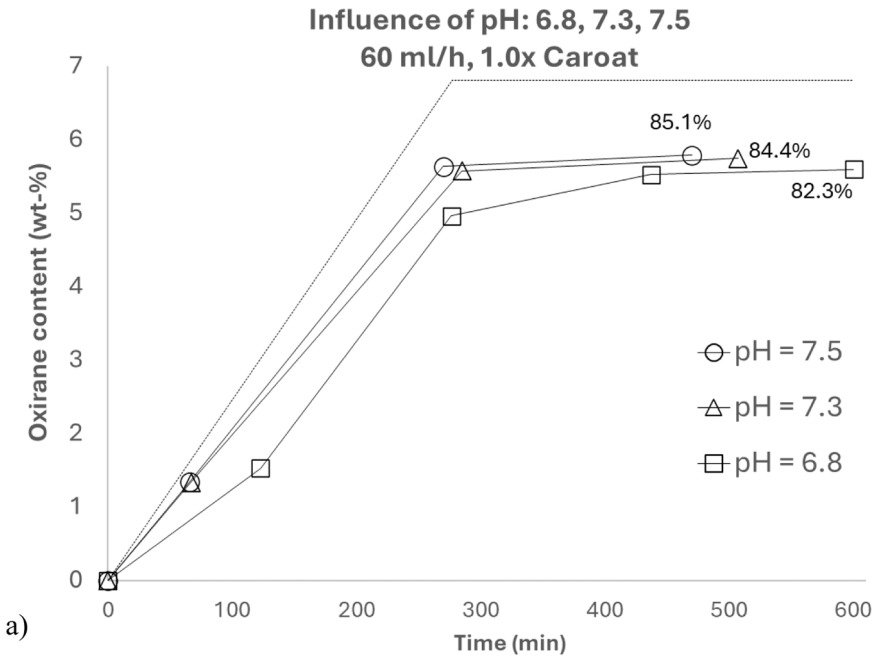
The pH should be kept at a high enough level (pH > 6) in order to favor the formation of the reactive intermediate DMDO. Since the triple salt compound itself, as a water solution, is acidic, the pH must be brought to the desired level by continuous addition of KOH. However, the pH cannot be too high, either, since the vegetable oil is sensitive for saponification. Therefore, as a standard praxis, the pH was usually kept at the level 6.80. Some experiments were, however, performed to study the possibility to increase the oxirane yield by increasing the pH by a slight margin (Fig. 11). The experiments were studied with the standard feed rate 60 ml/h, and the slowest feed rate 30 ml/h, with the Caroat to DB ratio 1:1 and 1.2:1, and the higher pH levels were 7.3 and 7.7.

As shown in Fig. 11, increasing the pH slightly improves the final oxirane yield. At 60 ml/h Caroat feed and 1.0 × dosage (Fig. 11a), a modest increase in final oxirane content is observed when the pH is raised from 6.8 to 7.5. However, when comparing intermediate values (at 260–280 min), the reaction rate is clearly enhanced at higher pH, even though the final yields remain relatively close. Based on this, it was hypothesized that combining a slower Caroat feed with elevated pH could improve both conversion and selectivity. This was confirmed in experiments using the slowest feed rate (30 ml/h), 20% excess Caroat (1.2 ×), and pH 7.7, which gave the highest oxirane yield in this study—95.4% (Fig. 11b).

3.4. Performance comparison with prilezhaev and enzymatic epoxidation

The maximum oxirane yield obtained in this study (95.4%) is comparable to the highest conversions reported for conventional Prilezhaev epoxidation using in situ generated performic acid (Campanella et al., 2008) and for chemo-enzymatic lipase-based systems (Törnvall et al., 2007; Aguilera et al., 2022).

However, percarboxylic acid–based epoxidation systems are characterized by strongly exothermic reaction networks involving perhydrolysis, epoxidation and consecutive ring-opening and peroxide decomposition reactions. Thermal risk assessment studies on performic acid epoxidation have demonstrated that adiabatic temperature rises may exceed 200 °C and that time-to-maximum rate values under adiabatic conditions can fall below 8 h, indicating significant runaway



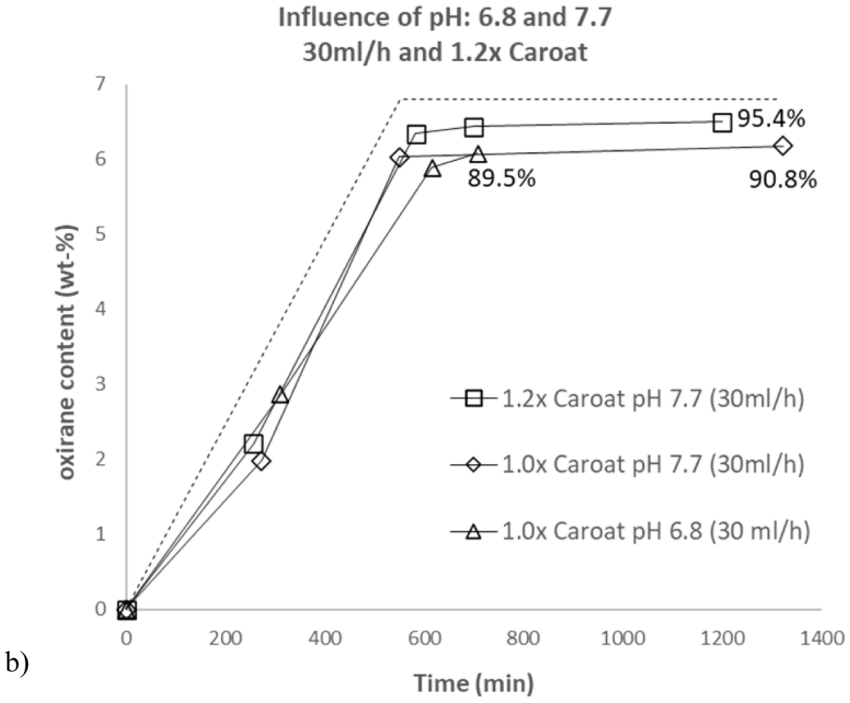


Fig. 11. a) Effect of pH (6.8, 7.3, 7.5) on epoxidation yield at fixed 1.0x Caroat and 60 ml/h feed rate. The endpoint values represent epoxide yield (wt%) relative to theoretical maximum (6.80 wt%) based on full conversion; b) the effect of pH (6.8, 7.7) under different Caroat loadings (1.0x and 1.2x) at 30 ml/h feed rate. Higher pH slightly improved final epoxide yield, particularly at 1.2x Caroat dosage.

potential (Leveneur et al., 2018). Furthermore, global sensitivity analyses have shown that the severity and probability of thermal runaway are highly sensitive to hydrogen peroxide concentration and cooling conditions (Garcia-Hernandez et al., 2022).

In contrast, the Caroat–acetone system operates at mild temperatures (25–30 °C) and near-neutral pH, reducing corrosion risks and limiting acid-catalyzed oxirane ring opening. The controlled semibatch oxidant dosing strategy enables regulation of reactive intermediate concentration and moderates heat release within the reactor. From a reactor engineering perspective, this concentration management provides an inherent safety advantage and facilitates scale-up by decoupling oxidant addition from peak heat evolution, while maintaining conversion levels comparable to dominant epoxidation technologies.

4. Kinetic and reactor modeling

Before presenting the kinetic model, several key assumptions about the reaction system are stated. The reacting mixture was considered homogeneous and well mixed throughout the experiment due to continuous mechanical stirring and absence of visible phase separation. A constant density was assumed in the model. Based on literature data, the density of native rapeseed oil (~0.91 g/cm^3) increases only slightly

upon full epoxidation (~0.94–0.96 g/cm^3), and this change is further moderated by the presence of large quantities of acetone, which reduces both the density and viscosity of the mixture. Similarly, while the viscosity of fully epoxidized oil is known to increase significantly (compared to native oil), the solvent effect of acetone leads to a well-fluidized, Newtonian-like system during the entire reaction. Therefore, viscosity and transport properties were assumed constant and non-limiting for the modeling scope. Although the reaction is mildly exothermic, the reactor was operated at a controlled temperature range of 25–30 °C with sufficient heat exchange to maintain near-isothermal conditions. Consequently, temperature effects were not included in the model and all kinetic data are considered valid under these uniform conditions.

4.1. Reaction mechanism and rate equations

The epoxidation mechanism is complicated, as sketched in Figs. 1–2. Acetone (B) reacts with the peroxy salt (A) forming an intermediate complex (I_1), which is transformed to a second intermediate (I_2) via a reaction with alkali (OH). Water (W) is released in this step. The second intermediate (I_2) rearranges to a reactive, cyclic intermediate (I) and dipotassium sulphate (K_2SO_4, S) is formed as a stoichiometric component. In the final step, the cyclic intermediate (I) reacts with the double bond(s) of the vegetable oil (C) giving the saturated product (P) and recovering acetone (B). Based on the scheme displayed in Fig. 2, the reaction sequence can be written as

$$A + B \rightleftharpoons I_1 \quad \text{(I)}$$

$$I_1 + OH \rightleftharpoons I_2 + W \quad \text{(II)}$$

$$I_2 \rightleftharpoons S + I \quad \text{(III)}$$

$$\underline{I + C \rightleftharpoons P + B} \quad \text{(IV)}$$

$$A + C + OH \rightleftharpoons P + S + W$$

The overall reaction is a consecutive process; the reaction of the oil, peroxy salt and alkali gives the saturated compound, K_2SO_4, and water. Acetone plays the role of a catalyst.

There are different ways to derive the rate equation based on this plausible mechanism. One approach is to assume that some of the reaction steps are rapid while other ones are slow, rate determining steps. The well-known quasi-equilibrium hypothesis can then be applied to the rapid steps, and the rate constants of these steps are eliminated. However, for this particular case it is not self-evident to conclude, which steps are rapid, which ones rate determining. From a chemical viewpoint, it could be speculated that the second step might be more rapid than the other ones, because it involves a single proton change only. On the other hand, the rearrangement (3) and double bond epoxidation (4) steps might be slower than the other steps in the mechanism.

Based on this discussion, it is better to start from the more general hypothesis, namely the quasi-stationary principle in deriving the rate expression for the overall process. According to the principle of quasi-stationarity, the generation rates of the intermediates are approximated to zero, since these compounds are formed and destroyed rapidly ($r_I \sim 0$). The rate expressions of the elementary reaction steps are obtained in a straightforward manner,

$$r_1 = a_1 - a_{-1}\, c_{I1} \quad (1)$$

$$r_2 = a_2\, c_{I1} - a_{-2}\, c_{I2} \quad (2)$$

$$r_3 = a_3\, c_{I2} - a_{-3}\, c_I \quad (3)$$

$$r_4 = a_4 c_I - a_{-4} \quad (4)$$

where $a_1 = k_1 c_A c_B$, $a_{-1} = k_{-1}$, $a_2 = k_2 c_{OH}$, $a_{-2} = k_2 c_W$, $a_3 = k_3$, $a_{-3} = k_{-3} c_S$, $a_4 = k_4 c_C$, and $a_{-4} = k_{-4} c_B c_P$.

A closer examination of the reaction stoichiometry reveals that the generation rates of the intermediates can be expressed by

$$r_{I1} = r_1 - r_2 \quad (5)$$

$$r_{I2} = r_2 - r_3 \quad (6)$$

$$r_I = r_3 - r_4 \quad (7)$$

All of these rates are approximated to zero according to the stationary state hypothesis, thus the following equation system is obtained,

$$r_1 - r_2 = r_2 - r_3 = r_3 - r_4 = 0 \quad (8)$$

which implies that $r_1 = r_2 = r_3 = r_4 = r$, where r de facto gives the rate of the overall reaction. Now, the mathematical machinery can be sent to operation. After inserting all the rate expressions, we get a linear algebraic equation system with respect to the intermediates (I_1, I_2, I). An elimination procedure is applied as follows, sequentially for steps 1–2 and 3–4, respectively,

$$a_2\, r = a_1 a_2 - a_{-1} a_2 c_{I1}$$

$$a_{-1}\, r = a_{-1} a_2 c_{I1} - a_{-1}\, a_{-2}\, c_{I2}$$

$$(a_2 + a_{-1})\, r = a_1 a_2 - a_{-1}\, a_{-2}\, c_{I2} \quad (9)$$

$$a_4\, r = a_3\, a_4 c_{I2} - a_{-3}\, a_4\, c_I$$

$$a_{-3}\, r = a_{-3}\, a_4\, c_I - a_{-3}\, a_{-4}$$

$$(a_4 + a_{-3})\, r = a_3\, a_4\, c_{I2} - a_{-3}\, a_{-4} \quad (10)$$

From the remaining Eqs. (9) and (10), the intermediate (I_2) concentration can be eliminated, and an explicit expression for the reaction rate is easily obtained,

$$r = \frac{a_1 a_2 a_3 a_4 - a_{-1} a_{-2} a_{-3} a_{-4}}{a_2 a_3 a_4 + a_{-1} a_3 a_4 + a_{-1} a_{-2} a_4 + a_{-1} a_{-2} a_{-3}} \quad (11)$$

By inserting the original definitions of $a_1 \ldots a_{-4}$, the rate equation becomes

$$r = \frac{(k_1 k_2 k_3 k_4 c_A c_{OH} c_C - k_{-1} k_{-2} k_{-3} k_{-4} c_W c_S c_P) c_B}{k_2 k_3 k_4 c_{OH} c_C + k_{-1} k_3 k_4 c_C + k_{-1} k_{-2} k_4 c_W c_C + k_{-1} k_{-2} k_{-3} c_W c_S} \quad (12)$$

Recalling that the overall equilibrium constant of the process is

$$K = \frac{k_1 k_2 k_3 k_4}{k_{-1} k_{-2} k_{-3} k_{-4}} \quad (13)$$

and merging the forward rate constants, $k = k_1 k_2 k_3 k_4$, the rate equation is transformed to

$$r = \frac{k c_B (c_A c_C c_{OH} - c_P c_W c_S / K)}{k_2 k_3 k_4 c_{OH} c_C + k_{-1} k_3 k_4 c_C + k_{-1} k_{-2} k_4 c_W c_C + k_{-1} k_{-2} k_{-3} c_W c_S} \quad (14)$$

By division the nominator and denominator by $k_2 k_3 k_4$, the rate equation can be rewritten to

$$r = \frac{k'' c_B (c_A c_C c_{OH} - c_P c_W c_S / K)}{(\alpha_1 + c_{OH}) c_C + (\alpha_2 c_C + \alpha_3 c_S) c_W}, \; k'' = k_1 \quad (15)$$

where

$$\alpha_1 = \frac{k_{-1}}{k_2} \quad (16)$$

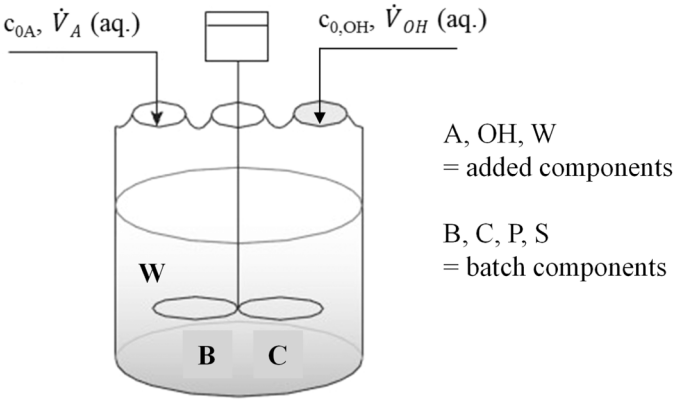


Fig. 12. Summary of the modeling principles.

$$\alpha_2 = \frac{k_{-1}k_{-2}}{k_2 k_3} \tag{17}$$

$$\alpha_3 = \frac{k_{-1}k_{-2}k_{-3}}{k_2 k_3 k_4} \tag{18}$$

This rate equation contains quite many adjustable parameters, and thus some simplifications are highly welcome. If step 3 is assumed to be slow compared to step 1, α_2 becomes the dominating term and the rate equation becomes

$$r = \frac{k'' c_B (c_A c_C c_{OH} - c_P c_W c_S / K)}{\alpha_2 c_W c_C} \tag{19}$$

On the other hand, if step 3 is rapid compared to the other steps, the second term in the denominator of Eq. (15) is assumed to be negligible, and the rate equation takes the form

$$r = \frac{k'' c_B (c_A c_C c_{OH} - c_P c_W c_S / K)}{(\alpha_1 + c_{OH}) c_C} \tag{20}$$

In general, the equilibrium is presumed to be strongly shifted towards the products and thus $K \to \infty$. By considering this hypothesis, the simplified rate Eqs. (19) – (20) become

$$r = \frac{k'' c_B c_A c_{OH}}{\alpha_2 c_W} \tag{21}$$

$$r = \frac{k'' c_B c_A c_{OH}}{\alpha_1 + c_{OH}} \tag{22}$$

If step 4 is rate determining, α_1 and α_2 are assumed to be negligible, and the rate equation becomes

$$r = \frac{k'' c_B c_A c_C c_{OH}}{c_{OH} c_C + \alpha' c_S c_W} \tag{23}$$

where $\alpha' = \alpha_3$. Alternatively, if $\alpha_1 >> c_{OH}$, and α_2 is small, we get

$$r = \frac{k''' c_B c_A c_C c_{OH}}{\alpha' c_S c_W + c_C} \tag{24}$$

where $\alpha' = \alpha_3 / \alpha_1$. The ultimate simplification is to use directly the law of mass action, which gives

Table 1
Parameter estimation results.

Parameter	value
k'	0.395
k''	0.026
ϰ	1.0

$$r = k' c_B c_A c_C c_{OH} \tag{25}$$

Thus five rival rate models, Eqs. (21)-(25) can be compared. The models contain two adjustable kinetic parameters, except the last one which has only one parameter. It should be noticed, that c_{OH} = constant in the actual case, since the pH of the solution was kept constant. This implies that models (23) and (24) are indistinguishable with the present kinetic data. In practice the terms in the denominators (including c_C and $c_S c_W$) compensate to some degree each other during the progress of the reaction which implies that the denominator does not change that much and the mechanistic model approaches Eq. (25).

Some part of Caroat (A) is believed to decompose to unknown products or be consumed via unproductive side reactions. Although the exact decomposition mechanism was not measured, its effect was accounted for in the kinetic model. The disappearance of Caroat was described using a simple expression:

$$r'' = k'' c_A^{\varkappa} \tag{26}$$

where κ is an empirical exponent. The model provided a satisfactory fit to the experimental data, supporting the assumption of apparent first-order or pseudo-first-order behavior under the given conditions.

Possible side reactions of the epoxide, such as ring-opening reactions, were not modeled explicitly due to their minor contribution under the mildly alkaline and near-neutral reaction conditions used. Any losses in epoxidation efficiency were instead captured through the oxidant decomposition term (Eq. 26), which accounts for unproductive Caroat consumption and overall yield loss.

4.2. Component generation rates

Based on the stoichiometric scheme (Fig. 2), the component generation rates can be written in a straightforward manner,

$$r_A = -r - r'' \tag{27}$$

$$r_B = 0 \text{ (acetone is a catalyst)} \tag{28}$$

$$r_C = -r \tag{29}$$

$$r_S = +r \tag{30}$$

$$r_P = +r \tag{31}$$

$$r_W = +r \tag{32}$$

$$r_{OH} = 0 (c_{OH} \text{ was kept constant by controlled addition}) \tag{33}$$

4.3. Mass balances in semibatch reactor

The modelling principles are illustrated by Fig. 12.

Since the chemical system was dominated by the aqueous acetone phase, a pseudo-homogeneous approach is applied and only one phase is considered in the reactor modelling. Because of vigorous stirring, complete backmixing can be assumed for the isothermal semibatch tank reactor. The peroxysalt solution (A, Caroat) was fed into the reactor vessel with a constant volumetric flow rate, while the KOH solution (OH) was added in a controlled manner to keep the solution pH constant. The dynamic mass balances of the components can thus be written as follows,

$$\frac{dn_A}{dt} = c_{0A} \dot{V}_A + r_A V \tag{34}$$

$$\frac{dn_B}{dt} = r_B V \tag{35}$$

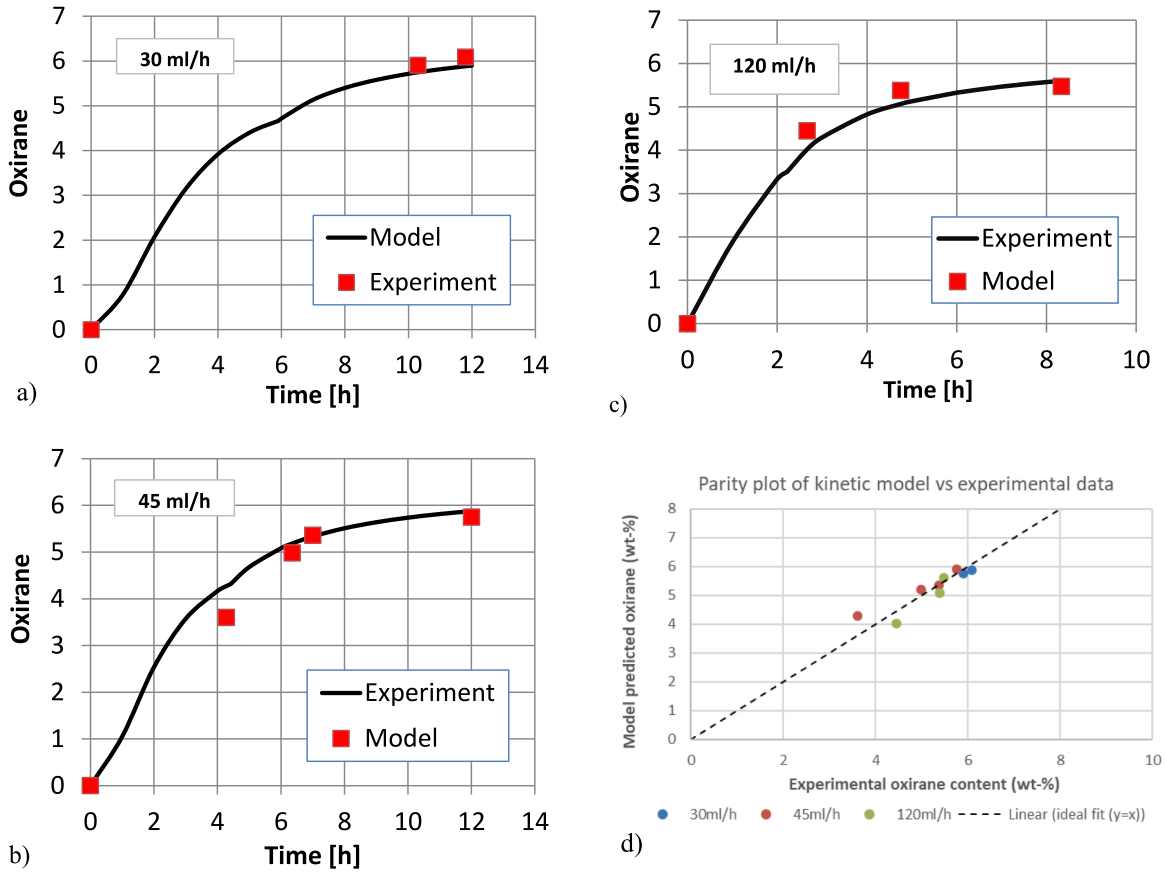


Fig. 13. a-c. Data fitting of the model with experimental data from experiments where the Caroat feed rate has been 30 ml/h, 45 ml/h, and 120 ml/h, d) Parity plot to show goodness-of-fit of the kinetic model.

$$\frac{dn_C}{dt} = r_C V \tag{36}$$

$$\frac{dn_{OH}}{dt} = c_{0,OH}\dot{V}_{OH} + r_{OH}V \tag{37}$$

$$\frac{dn_P}{dt} = r_P V \tag{38}$$

$$\frac{dn_S}{dt} = r_S V \tag{39}$$

$$\frac{dn_W}{dt} = c_{0,W}\dot{V}_{OH} + c'_{0,W}\dot{V}_A + r_W V \tag{40}$$

The symbols are defined in Notation. The liquid volume (V) increases with time following the formula

$$V = V_0 + \dot{V}_A t + \int_0^t \dot{V}_{OH} dt, \mathrm{t} \le \mathrm{t_{feed}} \tag{41}$$

$$V = V_0 + \dot{V}_A t_{feed} + \int_0^t \dot{V}_{OH} dt, \mathrm{t} > \mathrm{t_{feed}} \tag{42}$$

where t_{feed} is the feeding time of the peroxy salt (A) solution. The amounts of substance (n_i) are related to concentrations (c_i) by

$$n_i = c_i V \tag{43}$$

Differentiation of Eq. (43) gives

$$\frac{dn_i}{dt} = V\frac{dc_i}{dt} + c_i\frac{dV}{dt} \tag{44}$$

The derivative of the liquid volume is expressed with the volumetric flow rates

$$\frac{dV}{dt} = \dot{V}_A + \dot{V}_{OH} \tag{45}$$

Thus the derivative of the amount of substance becomes

$$\frac{dn_i}{dt} = V\frac{dc_i}{dt} + c_i(\dot{V}_A + \dot{V}_{OH}) \tag{46}$$

This expression is inserted in balance Eqs. (34) - (40). After some rearrangements we obtain for the batch (i = B, C, P, S) and semibatch (j = A, OH, W) components the final forms of the mass balance equations

$$\frac{dc_i}{dt} = r_i - \frac{c_i(\dot{V}_A + \dot{V}_{OH})}{V} \tag{47}$$

$$\frac{dc_j}{dt} = r_j - \frac{c_j(\dot{V}_A + \dot{V}_{OH})}{V} + \frac{c_{0j}\dot{V}_{OH} + c'_{0j}\dot{V}_A}{V} \tag{48}$$

It should be observed that $c_{0A} = 0$, $c'_{0A} > 0$, $c_{OH} > 0$, $c'_{OH} = 0$, $c_{0\,W} > 0$ and $c'_{0\,W} > 0$. The balance equation of KOH (OH) was omitted because the pH was maintained constant throughout the experiments. Also the mass balance of acetone (B) was discarded since acetone acts as a catalyst and its generation rate was zero. The liquid volume (V) was also updated by taking into account the sampling.

The initial conditions are known for all components, i.e. $c_i(t = 0)$ and $c_j(t = 0)$. The mathematical model consists of five ordinary differential equations (ODEs, initial value problem for A, C, P, S, W), which was solved numerically with a stiff ODE solver based on the backward difference method (BD) during the estimation of kinetic parameters from Eqs. (47) - (48).

The ODE system was solved repeatedly until the minimum of the

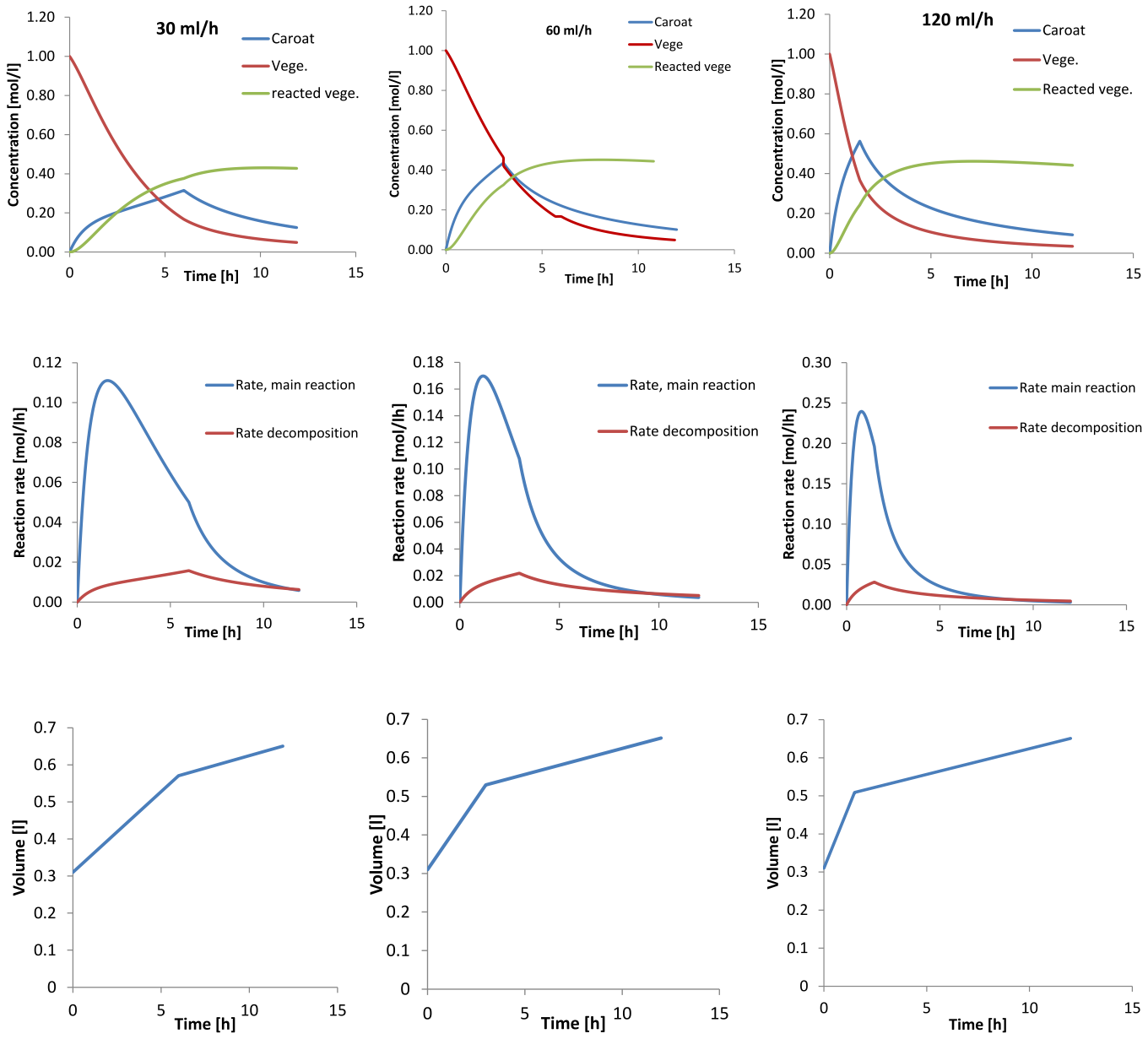


Fig. 14. Simulation of the reactor performance for various feed rates (30, 60, 120 ml/h) and 50 wt.-% excess of Caroat. The simulation is presented on a molar concentration basis for all key species (DB, Caroat, and oxirane), rather than using derived values like iodine number or oxirane wt.-%. Upper row: the concentration profiles for the vegetable oil (C), reacted vegetable oil and Caroat; middle row: the reaction rates for epoxidation and ring opening (decomposition); bottom row: the total reactor volume profiles.

objective function

$$Q = \sum (c_{p,\mathrm{exp}} - c_p)^2 \tag{49}$$

was reached. In Eq. (49), $c_{p,exp}$ and c_p refer to the experimentally measured and modelled concentrations, respectively. A combined simplex-Levenberg-Marquardt algorithm was used in the minimization of the objective function in the search of the optimal parameter values. The software Modest (Haario 2007) and gPROMS was used in calculations. In general, the computations run smoothly, without any significant difficulties.

4.4. Modelling results

Preliminary considerations of the experimental data revealed that the reaction rate is dependent on the concentrations of all the participating reactants and thus the model Eqs. (21)-(22) can be ruled out. Because of the compensation effect of the product and reactant concentrations, the predictions of Eqs. (23)-(24) on one hand and those of Eq. (25) on the other hand became very similar. By approximating the denominators to be constant in Eqs. (23)-(24), the simple expression (25) is obtained and it was used in the final parameter estimation. The decomposition of Caroat (A) was successfully described with first order kinetics (Eq. 26).

The parameter estimation results are collected in Table 1, and the fit of the model to the experimental data is shown in Fig. 13. The parameters became rather well determined, i.e. the standard errors were in most cases moderate. The fit of the model to the experimental data was excellent as demonstrated by Fig. 13. The discontinuities in the derivatives of the simulated curves are caused by the stop of the Caroat (A) feed.

To further evaluate the predictive accuracy of the kinetic model, a

parity plot was constructed comparing modeled and experimental oxirane values across the fitted experiments (Fig. 13d). The parity plot confirms good agreement, with a mean absolute percentage error of 5.4%.

Based on the validated kinetic model, simulation scenarios were conducted to investigate the influence of different Caroat feed rates on epoxidation performance. These are presented in Fig. 14. A Caroat excess of 1.5 × was used in all cases to examine the system's behavior beyond the experimental range and to explore the benefits of increased oxidant availability. The simulations show the expected trends: disappearance of double bonds, formation of the epoxide product, and the gradual decomposition of Caroat. Once Caroat addition is complete, its concentration declines due to unproductive degradation and residual reaction activity.

The modeled concentrations are presented on a molar basis, with the initial double bond concentration normalized to 1.00 mol/L. This corresponds to a starting oil concentration of approximately 0.43 mol/L, based on the assumption of three double bonds per triglyceride and a total reactor volume of ~1.29 L. As a result, the maximum oxirane concentration appears to plateau below 0.5 mol/L — a feature reflecting dilution rather than incomplete conversion. Additionally, the slight decline in oxirane concentration toward the end of the reaction is not due to ring-opening (which is not included in the model) but is instead an effect of ongoing KOH addition, which increases reactor volume and thereby reduces concentration on a per-liter basis.

Overall, the simulation results highlight the trade-off between reaction rate and oxidant efficiency: higher feed rates accelerate epoxidation but increase oxidant loss through decomposition, whereas slower feed rates enhance selectivity by prolonging oxidant availability.

5. Conclusions

Kinetic experiments of vegetable oil epoxidation using Caroat as the oxidant were performed in a laboratory-scale semibatch reactor. Acetone served both as the solvent and ketone component for in situ generation of the reactive DMDO intermediate. The main objective was to maximize the oxirane yield of the oil while minimizing side reactions, and improving oxidant utilization and volume efficiency.

A comprehensive parameter study was carried out, focusing on the Caroat-to-double bond molar ratio, oxidant feed rate, and the pH level. The results demonstrated that the oxidant losses occurred either through decomposition or formation of volatile intermediates escaping from the reactor, leading to reduced effective epoxidation. By decreasing the oxidant feed rate, significantly higher oxirane yields were achieved. Additionally, increasing the Caroat excess and operating at moderately elevated pH improved oxirane formation, although excessive alkalinity must be avoided to prevent side reactions. Under optimized conditions (20% excess Caroat, 30 ml/h feed rate, pH 7.7), the final oxirane yield reached 95.4%, representing the highest yield achieved in this study. This level of conversion is comparable to the highest yields reported for conventional Prilezhaev epoxidation using in situ generated peracids and for chemo-enzymatic epoxidation systems, while offering improved control of oxidant dosing and reduced risks associated with peracid handling.

The experimental results were successfully incorporated into a mathematical model describing the complex multiphase reaction kinetics in the laboratory-scale semibatch reactor. The kinetic parameters were estimated reliably, and the validated model enables prediction of the system behavior under various operating conditions, providing a useful tool for process optimization and future scale-up studies.

CRediT authorship contribution statement

Pasi Tolvanen: Writing – original draft, Visualization, Validation, Methodology, Investigation, Formal analysis, Data curation, Conceptualization. **Kari Eränen:** Validation, Supervision, Resources, Project administration, Methodology, Investigation, Conceptualization. **Teuvo Kilpiö:** Writing – original draft, Visualization, Validation, Methodology, Investigation, Formal analysis. **Tapio Salmi:** Writing – original draft, Visualization, Validation, Supervision, Project administration, Methodology, Investigation, Funding acquisition, Formal analysis, Conceptualization. **Johan Wärnå:** Validation, Supervision, Software, Methodology, Investigation, Formal analysis. **Adriana Freites:** Writing – original draft, Validation, Supervision, Software, Methodology, Investigation, Conceptualization.

Declaration of Competing Interest

The authors declare that they have no known competing financial interests or personal relationships that could have appeared to influence the work reported in this paper.

Acknowledgement

The work is a part of the activities of Johan Gadolin Process Chemistry Centre (PCC) at Åbo Akademi University. The financial support from Raisio Oyj (P. Tolvanen) and Academy of Finland (T. Salmi) are gratefully acknowledged.

Appendix A. Supporting information

Supplementary data associated with this article can be found in the online version at doi:10.1016/j.cherd.2026.03.002.

References

Adhvaryu, A., Erhan, S.Z., 2002. Epoxidized soybean oil as a potential source of high-temperature lubricants15.

Aguilera, A.F., Lindroos, P., Rahkila, J., Klimov, M.M., Tolvanen, P., Salmi, T., 2022. Lipase catalyzed green epoxidation of oleic acid using ultrasound as a process intensification method. Chem. Eng. Process. Process. Intensif. 174. https://doi.org/10.1016/j.cep.2022.108882.

Aguilera, A.F., Tolvanen, P., Eränen, K., Wärnå, J., Leveneur, S., Marchant, T., et al., 2019. Kinetic modelling of Prileschajew epoxidation of oleic acid under conventional heating and microwave irradiation. Chem. Eng. Sci. 199, 426–438. https://doi.org/10.1016/j.ces.2019.01.035.

Aguilera, A.F., Tolvanen, P., Heredia, S., Muñoz, M.G., Samson, T., Oger, A., et al., 2018. Epoxidation of fatty acids and vegetable oils assisted by microwaves catalyzed by a cation exchange resin. Ind. Eng. Chem. Res. 57, 3876–3886. https://doi.org/10.1021/acs.iecr.7b05293.

Campanella, A., Baltanás, M.A., 2007. Degradation of the oxirane ring of epoxidized vegetable oils in a liquid-liquid-solid heterogeneous reaction system. Chem. Eng. Process. Process.Intensif. 46, 210–221. https://doi.org/10.1016/j.cep.2006.06.001.

Campanella, A., Fontanini, C., Baltanás, M.A., 2008. High yield epoxidation of fatty acid methyl esters with performic acid generated in situ. Chem. Eng. J. 144, 466–475. https://doi.org/10.1016/j.cej.2008.07.016.

Campanella, A., Rustoy, E., Baldessari, A., Baltanás, M.A., 2010. Lubricants from chemically modified vegetable oils. Bioresour. Technol. 101, 245–254. https://doi.org/10.1016/j.biortech.2009.08.035.

Funck, L.G., Barrera-Arellano, Daniel, Block, J.M., 2006. Servicios personalizados revista. Arch. Lat. Nutr. 56, 123–134.

Garcia-Hernandez, E.A., Elmoukrie, M.E., Leveneur, S., Gourich, B., Vernieres-Hassimi, L., 2022. Global sensitivity analysis to identify influential model input on thermal risk parameters: to cottonseed oil epoxidation. J. Loss Prev. Process Ind. 77. https://doi.org/10.1016/j.jlp.2022.104795.

Goering, C.E., Schwab, A.W., Daugherty, M.J., Pryde, E.H., Heakin, A.J., 1982. Fuel Prop. Elev. Veg. Oils.

Goud, V.V., Patwardhan, A.V., Dinda, S., Pradhan, N.C., 2007a. Epoxidation of karanja (Pongamia glabra) oil catalysed by acidic ion exchange resin. Eur. J. Lipid Sci. Technol. 109, 575–584. https://doi.org/10.1002/ejlt.200600298.

Goud, V.V., Patwardhan, A.V., Dinda, S., Pradhan, N.C., 2007b. Kinetics of epoxidation of jatropha oil with peroxyacetic and peroxyformic acid catalysed by acidic ion exchange resin. Chem. Eng. Sci. 62, 4065–4076. https://doi.org/10.1016/j.ces.2007.04.038.

Hanif, M., Zahoor, A.F., Saif, M.J., Nazeer, U., Ali, K.G., Parveen, B., et al., 2024. Exploring the synthetic potential of epoxide ring opening reactions toward the synthesis of alkaloids and terpenoids: a review. RSC Adv. 14, 13100–13128. https://doi.org/10.1039/d4ra01834f.

Hilker, I., Bothe, D., Pruk, J., Warnecke, H.-J., 2001. Chemo-enzymatic epoxidation of unsaturated plant oils56.

Lämsä, M., Kosonen, K., 2012. Process Epoxydation Veg. Oils WO2012098295A1 Pat.

Lathi, P.S., Mattiasson, B., 2007. Green approach for the preparation of biodegradable lubricant base stock from epoxidized vegetable oil. Appl. Catal. B 69, 207–212. https://doi.org/10.1016/j.apcatb.2006.06.016.

Leveneur, S., Pinchard, M., Rimbault, A., Safdari Shadloo, M., Meyer, T., 2018. Parameters affecting thermal risk through a kinetic model under adiabatic condition: application to liquid-liquid reaction system. Thermochim. Acta 666, 10–17. https://doi.org/10.1016/j.tca.2018.05.024.

Meng, Y., Taddeo, F., Aguilera, A.F., Cai, X., Russo, V., Tolvanen, P., et al., 2021. The lord of the chemical rings: catalytic synthesis of important industrial epoxide compounds. Catalysts 11. https://doi.org/10.3390/catal11070765.

Mohammed, M.L., Saha, B., 2022. Recent advances in greener and energy efficient alkene epoxidation processes. Energies 15. https://doi.org/10.3390/en15082858.

Santacesaria, E., Tesser, R., Di Serio, M., Turco, R., Russo, V., Verde, D., 2011. A biphasic model describing soybean oil epoxidation with H2O2 in a fed-batch reactor. Chem. Eng. J. 173, 198–209. https://doi.org/10.1016/j.cej.2011.05.018.

Saurabh, T., 2011. PBSLMRVC. epoxidation of vegetable oils: a review. Int. J. Adv. Eng. Technol. 2, 491–501.

Shu, L., Shi, Y., 2000. An efficient ketone-catalyzed epoxidation using hydrogen peroxide as oxidant. J. Org. Chem. 65, 8807–8810. https://doi.org/10.1021/jo001180y.

Törnvall, U., Orellana-Coca, C., Hatti-Kaul, R., Adlercreutz, D., 2007. Stability of immobilized Candida antarctica lipase B during chemo-enzymatic epoxidation of fatty acids. Enzym. Microb Technol. 40, 447–451. https://doi.org/10.1016/j.enzmictec.2006.07.019.